Archives Italiennes de Biologie, 150: 194-217, 2012.

A subcellular analysis of genetic modulation of PINK1 on mitochondrial alterations, autophagy and cell death

P. LENZI[1*], R. MARONGIU[2#], A. FALLENI[1], V. GELMETTI[2], C.L. BUSCETI[3], S. MICHIORRI[2##], E.M. VALENTE[2,4§], F. FORNAI[1,3§]

[1] Department of Human Morphology and Applied Biology, University of Pisa, taly;
[2] Casa Sollievo della Sofferenza Hospital, CSS-Mendel Institute, San Giovanni Rotondo, Italy;
[3] Lab of Neurobiology of Movement Disorders, IRCCS, INM Neuromed Venafro (IS), Italy
[4] Department of Medical and Surgical Pediatric Sciences, University of Messina, Italy;
[#] Present address: Laboratory of Molecular Neurosurgery, Weill Cornell Medical College, New York, NY;
[##] 'GENOMA' Molecular Genetics Laboratory, Rome, Italy

ABSTRACT

Mutations in the PTEN-induced putative kinase1 (PINK1) represent the second most frequent cause of autosomal recessive Parkinson's disease. The PINK1 protein mainly localizes to mitochondria and interacts with a variety of proteins, including the pro-autophagy protein beclin1 and the ubiquitin-ligase parkin. Upon stress conditions, PINK1 is known to recruit parkin at the surface of dysfunctional mitochondria and to activate the mitophagy cascade. Aim of this study was to use a simple and highly reproducible catecholamine cell model and transmission electron microscopy to characterize whether PINK1 could affect mitochondrial homeostasis, the recruitment of specific proteins at mitochondria, mitophagy and apoptosis. Samples were analyzed both in baseline conditions and following treatment with methamphetamine (METH), a neurotoxic compound which strongly activates autophagy and produces mitochondrial damage. Our data provide robust sub-cellular evidence that the modulation of PINK1 levels dramatically affects the morphology and number of mitochondria and the amount of cell death. In particular, especially upon METH exposure, PINK1 is able to increase the total number of mitochondria, concurrently recruit beclin1, parkin and ubiquitin and enhance the clearance of damaged mitochondria. In the absence of functional PINK1 and upon autophagy stress, we observe a failure of the autophagy system at large, with marked accumulation of dysfunctional mitochondria and dramatic increase of apoptotic cell death. These findings highlight the strong neuroprotective role of PINK1 as a key protein in the surveillance and regulation of mitochondrial homeostasis.

Key words

Parkinson's Disease • Methamphetamine • Mitophagy • Beclin1 • Parkin

Abbreviations

ALV, autophagy-like vacuoles; ER, endoplasmic reticulum; METH, Methamphetamine; PD, Parkinson's disease; PINK1, PTEN-induced protein kinase 1; TEM, transmission electron microscopy.

Introduction

Parkinson's disease (PD) is a common neurodegenerative disorder due to the loss of catecholamine-containing neurons in the substantia nigra and other brain nuclei (Gelb et al., 1999; Braak et al., 2004). The pathological hallmark of PD is the presence of cytoplasmic protein aggregates, mainly constituted of alpha-synuclein, ubiquitin, and parkin (Shults, 2006). Two main mechanisms have been impli-

Corresponding Author: Francesco Fornai, MD, Department of Human Morphology and Applied Biology, University of Pisa, via Roma 55, I-56126 Pisa, Italy - Tel.: +39 50 2218601 - Fax: +39 50 2218606 - Email: francesco.fornai@med.unipi.it
[*] These two authors contributed equally to the work. [§] E.M.V and F.F. share last-authorship.

cated in the pathogenesis of PD: accumulation of misfolded proteins and mitochondrial dysfunction (Hardy, 2010) both of which are critically related to an impairment of the neuronal autophagy activity (Cherra et al., 2010; Xilouri and Stefanis, 2011).

Autophagy has been increasingly recognized as a major neuroprotective mechanism, that is constitutively active in the clearance of misfolded proteins and in the selective removal of dysfunctional mitochondria (mitophagy) (Metcalf et al., 2010; Youle and Narendra, 2011). Upon stress conditions, neuronal cells often respond with a marked increase of their autophagy rate, and defective autophagy may promote neuronal cell death (Isidoro et al., 2009).

Although most cases are sporadic, in a subset of patients PD is inherited as a mendelian trait due to mutations in specific genes (Lesage and Brice, 2009). Among them, PTEN-induced kinase 1 (PINK1) encodes for a mitochondrial kinase with multiple neuroprotective activities, that is especially aimed at maintaining mitochondrial homeostasis upon stressing conditions (Pogson et al., 2011; Valente et al., 2004). In particular, PINK1 has been recently shown to play a pivotal role in promoting selective mitophagy, by recruiting parkin on the surface of dysfunctional mitochondria (Matsuda and Tanaka, 2010; Narendra and Youle, 2011). In turn, parkin ubiquitinates several proteins of the outer mitochondrial membrane, promoting their degradation through the ubiquitin-proteasome pathway and recruiting pro-autophagy factors necessary for mitophagy to take place (Geisler et al., 2010a; Chan et al., 2011; Gegg and Schapira, 2011; Yoshii et al., 2011). Consistent with this, we found that PINK1 is able to promote autophagy and directly interacts with beclin1, a protein that is essential for initiation of the autophagy process (Michiorri et al., 2010).

Despite this plethora of data, there are contrasting evidences as to whether PINK1 mutations or silencing may actually increase or reduce mitophagy (Geisler et al., 2010b; Narendra et al., 2010; Cui et al., 2011). Moreover, it is still unclear whether the effects of PINK1 on the autophagy machinery are limited to the induction of mitophagy or if they extend to the autophagy process at large. These uncertainties may depend on the variety of experimental settings used within different studies, and the lack of extreme conditions to stress the autophagy/mitophagy machinery that would better reveal the critical role of PINK1 function for the fate of mitochondria and for cell survival.

To investigate this issue, in the present study we tested the effects of wild type (wt) or mutant PINK1 overexpression or PINK1 knock-down in a simple cell system, the catecholamine–containing PC12 cells, both in baseline conditions and following methamphetamine (METH) exposure. This compound induces neurotoxicity *in vivo*, and determines toxicity up to cell death in PC12 cells, which is associated with a dramatic induction of the autophagy machinery (Larsen et al., 2002). In this context, autophagy activation plays a compensatory role in counteracting METH-induced cell toxicity (Isidoro et al., 2009; Pasquali et al., 2009); in fact, upon autophagy impairment, even low METH doses are able to produce cell death, an effect that is rescued by the administration of autophagy inducers (Castino et al., 2008).

In this cell system, we employed transmission electron microscopy (TEM) to analyze the effects of manipulating PINK1 expression levels upon the total number and the percentage of damaged mitochondria, and the mitochondrial localization of key PINK1 interactors such as beclin1 and parkin, in addition to mitophagy signals such as ubiquitin. We also evaluated the number of plain autophagy vacuoles and those positive for the autophagy marker LC3, along with LC3-stained endomembranous structures. Finally, we related the association of these phenomena with the onset of apoptotic cell death.

Materials and Methods

Cell culture

The rat PC12 cell line was obtained from Sigma (Sigma-Aldrich, 88022401) and cultured in RPMI 1640 medium with 10% horse serum and 5% fetal bovine serum at 37°C in 95% humidifier air and 5% CO_2. For all the experiments, cells were seeded and cultivated for 24 h, and then transfected using Lipofectamine 2000 (Invitrogen, 11668-019) according to the manufacturer's instructions. Cells were studied both in baseline conditions (vehicle) and following exposure to Methamphetamine (METH - gently gifted from Prof. Giusiani, Forensic Medicine, University of Pisa). In particular, 24 hours

after transfection, cells were treated with METH at final concentration of 1 μM for 72h. Following treatment, the cells were further processed for the electron microscopy analysis.

Eukaryotic expression vectors

The PINK1 constructs were all tagged at C-terminus with the HA epitope. Wild type PINK1 and mutant PINK1^{W437X} were cloned in pcDNA3.1 and have been previously described (Silvestri et al., 2005). To analyze PINK1 expression, cells were transfected with pcDNA3.1 empty vector, PINK1wt-HA or PINK1^{W437X}- HA and harvested in 1% Triton-X lysis buffer at 48, and 96 hours post transfection. For each sample 40 μg of proteins were run on a SDS-PAGE and western blots were probed with rat anti-HA antibody (Roche Diagnostics, 11867423001) specific for the HA epitope tag.

Immunofluorescence analysis was performed as described previously (Michiorri et al., 2010) using the anti-HA antibody (Covance, Berkeley, CA) to detect PINK1 proteins. Primary antibody was visualized using the appropriate secondary antibody conjugated with Alexa Fluor 555 (Molecular Probes). Transfection efficiency was about 50-60% for both PINK1-FL and PINK1^{W437X} (Supplementary Fig. 1A). Expression levels of both PINK1 constructs remained stable and sustained up to 96 hours post-transfection, and were not affected by METH treatment (Supplementary Fig. 1B-C).

To knock-down endogenous rat PINK1 expression, the pSIH1-H1-copGFP vector carrying a shRNA (sense strand: GGAGCAGTTACTTACAGAAGA) against the rat PINK1 was used (gently gifted from Prof. Masliah, Department of Neurosciences, University of California San Diego).

To detect the efficiency of PINK1 gene silencing, we preferred to test the levels of PINK1 RNA by real time PCR, since anti-PINK1 commercial antibodies are not able to reliably detect the levels of endogenous protein by Western Blotting. For real time PCR, the siPINK1 or the scramble shRNA construct was transfected in PC12 cells and RNA was extracted with the RNeasy mini spin column kit (Qiagen, 74104) 48, 72 and 96 hours after transfection, according to the manufacturer's instructions. One microgram of RNA was retro-transcribed using the SuperScript® II Reverse Transcriptase (Invitrogen, 18064-014). PINK1 gene expression levels were measured by quantitative Real-Time PCR using a Power SYBR Green master mix and an ABI PRISM HT7900 Sequence Detection System (Applied Biosystem, 4402955M). Rat GAPDH gene was amplified as the housekeeping gene. Primers to amplify both rat PINK1 (Fw - GCAATGCCGCTGTGTATGAA; Rev - TGAGACGACATCTGGGCCTT) and rat GAPDH (Fw - GTTACCAGGGCTGCCTTCTC; Rev - GGGTTTCCCGTTGATGACC) were designed using Primer Express software. Relative expression was calculated using the ΔΔCt method. Supplementary Fig. 1D shows relative expression levels of PINK1 at 96 hours after transfection.

In all experiments performed in this work, we did not observe any differences between untransfected cells and cells overexpressing either pcDNA3.1 empty vector (control for PINK1wt and PINK1^{W437X} overexpression) or scramble shRNA (control for shPINK1).

Transmission Electron Microscopy (TEM)

Cells from each experimental group were centrifuged at 1.000 g for 5 min. After removal of the surnatant, each pellet was washed in PBS before being fixed.

Fixation

In a pilot series of experiments, we combined different concentrations of paraformaldehyde and glutaraldehyde in order to obtain the optimal fixing solution to perform immunoelectron microscopy, adding up to our previous validation studies (Fornai et al., 2001). When comparing different methods, the best fixing procedure for immunocytochemistry in our experimental setting was carried out with a solution containing 2.0% paraformaldehyde/0.1% glutaraldehyde in 0.1 M PBS (pH 7.4). In this way, the covering of antigen epitopes was minimal while the morphology of the tissue was preserved, despite a slight reduction in the electron density of sub-cellular structures. This method prevents the occurrence of specific TEM artifacts. In fact, it has been shown that high aldehydes concentrations in time determine TEM artifacts resembling autophagy vacuoles (Bowes and Maser, 1988) which could impair the detection of authentic autophagosomes (Fornai et al., 2001). Apart from the fixing solution, the time interval and temperature of fixation were carefully established at 1h and 4°C.

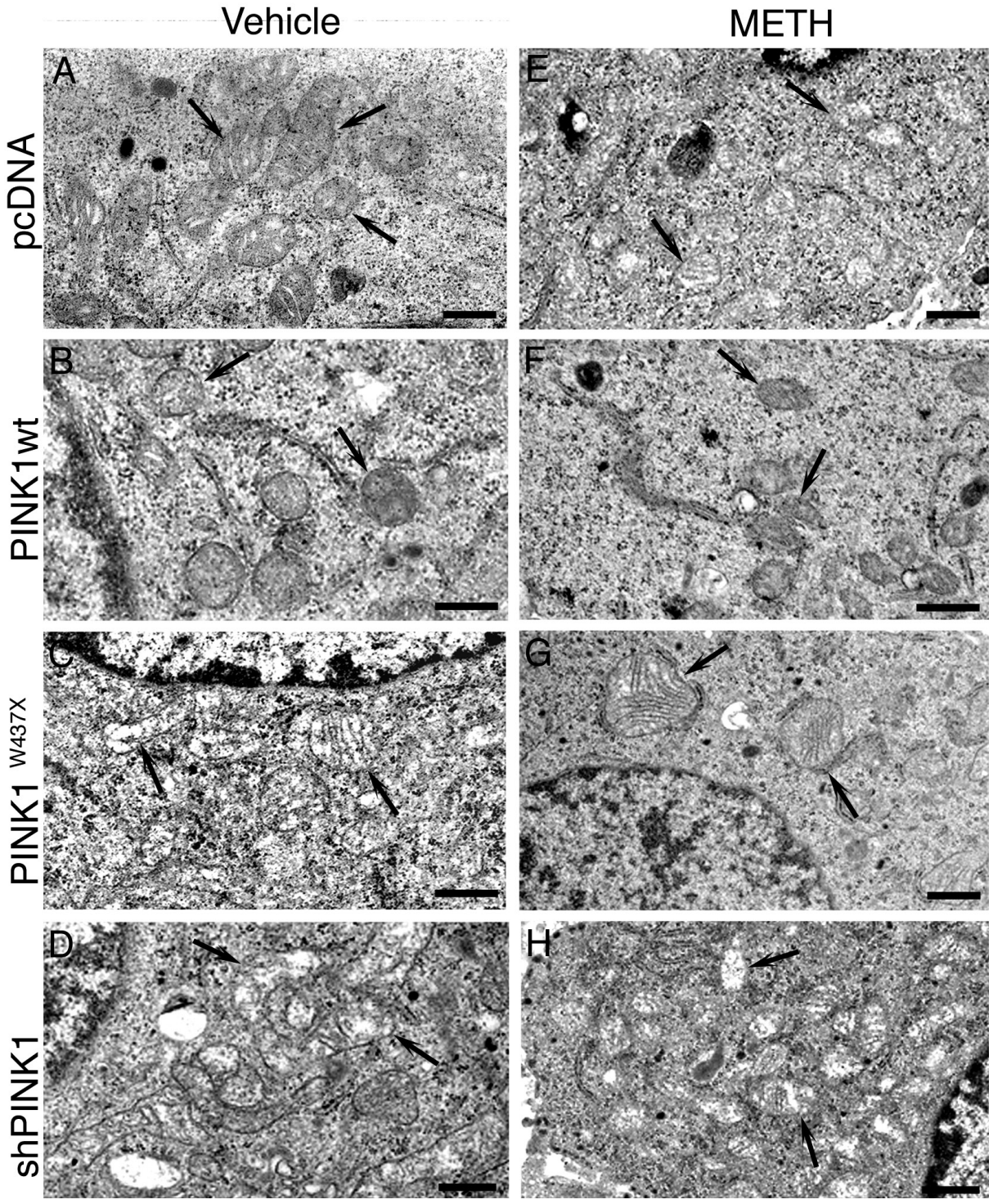

Fig. 1. - Representative ultrastructural mitochondrial changes induced by modulation of PINK1 expression. Micrographs represent the range of mitochondrial abnormalities observed upon PINK1 modulation in baseline conditions (A-D) and upon METH exposure (E-H). In each panel, arrows respectively show: A) well-preserved mitochondria with an electrondense matrix and well-arranged cristae; B) normal mitochondria with packed cristae and electrondense homogeneous matrix; C) mitochondrial alterations consisting of matrix dilution and several fragmented cristae; D) loss of mitochondria matrix together with disrupted and disarranged cristae; E) alterations in mitochondria matrix and cristae; F) well-conformed mitochondria; G) multiple cristae fragmentation; H) severe damage of mitochondrial architecture, in particular loss of matrix and disrupted cristae. pcDNA, PINK1wt and PINK1W437X: cells overexpressing pcDNA empty vector, wild type and mutant PINK1W437X, respectively; shPINK1: PINK1 silenced cells. Scale bars: 0.5 μm.

Post-fixation and embedding

The post-fixation was carried out in 1% OsO_4 for 1h at 4°C and specimens were then dehydrated in ethanol and embedded in epoxy resin. Ultrathin sections (40-50 nm) of cultured cells were cut at the ultramicrotome. Sections were contrasted with uranyl acetate (saturated solution in methanol) and lead citrate, and examined using a Jeol JEM SX 100 electron microscope (Jeol). As for the fixation, the post-fixing and embedding procedures were selected based on pilot studies and current literature in order to provide the best conditions for immunogold-based ultrastructural counting. We did not apply the routine method, consisting in immediate embedding of fixed and dehydrated specimens in acrylic resins, since such a procedure does preserve antigens but impairs the preservation of the fine morphological trim.

Since the use of only aldehydes does not clearly stain subcellular structures, we combined the aldehydic solutions fixation with a second fixing in OsO_4. Osmium enhances the contrasts of cellular compartments through the delineation of phospholipid membranes within the cytoplasm, as clearly stated in a review describing the gold standard of TEM in studying autophagy (Swanlund et al., 2010). The binding of osmium to cell membranes also impedes the formation of membranous artifacts mentioned above. Post-fixed samples were then embedded using epoxy resin. In our work, the use of epoxy resin, instead of acrylic resin such as LR White, was essential to preserve subcellular structures and to combine an optimal cell trim with an acceptable integrity of antigen epitopes (Bendayan and Zollinger, 1983; D'Alessandro et al., 2004).

The post-embedding was carried out collecting ultrathin sections on nickel grids and deosmicating them in aqueous saturated sodium metaperiodate ($NaIO_4$) for 15-30 minutes at room temperature. After three washes with PBS pH 7.4, ultrathin sections were processed for immunocytochemistry. The $NaIO_4$ was selected based on its ability as an oxidizing agent to attack the hydrophobic alkane side-chains of epoxy resin (Bendayan and Zollinger, 1983; Causton, 1984) making the sections more hydrophilic and allowing a better contact between immunogold-conjugated antibodies and the antigens exposed at the surface of the sections. The solution facilitates in this way to visualize specific localizations of the immunolabeled probe within a net context of cell integrity, and allows the counting of molecules within specific cell compartments.

Immunocytochemistry

Grids were treated with cold PBS containing 10% goat serum and 0.2% saponin to block non-specific antigenic sites for 20 minutes at room temperature. Following the blocking step, samples were incubated in two different conditions: a) with a single primary antibody, or b) with two primary antibodies in order to obtain a co-localization (parkin/beclin1 and beclin1/ubiquitin). The different primary antibodies were: rabbit anti-parkin (Millipore, AB5112) diluted 1:75; mouse anti-beclin1 (Santa Cruz Biotechnology Inc., sc-48341) diluted 1:10; rabbit anti-ubiquitin (Sigma, U5379) diluted 1:10; rabbit anti-LC3 (Santa Cruz Biotechnology Inc., sc-28266) diluted 1:10. Incubations were carried out in ice cold PBS containing 1% goat serum and 0.2% saponin in a humidified chamber overnight at 4°C.

Ultrathin sections were washed in cold PBS, incubated with appropriate gold (10 nm or 20 nm)-conjugated secondary antibody (BB International, EMGMHL 10 anti mouse, EMGAR 20 anti rabbit) diluted 1:10 in PBS containing 1% goat serum and 0.2% saponin for 1 hour, at room temperature.

After rising in PBS, grids were incubated with 1% of glutaraldehyde for 3 min, washed in distilled water, counterstained as described above and observed under the electron microscope. Control sections were obtained by omitting the primary antibody and incubating with the secondary antibody only.

Assessment of the mitochondrial number and morphology, autophagy-like vacuoles and apoptotic cells

Mean and SEM values corresponding to graphs in figures are presented in Supplementary Table.

In our experimental settings we took advantage from cellular pellets because ultrathin sections contain cells randomly oriented, which is an appropriate condition for quantitative calculation (Yla-Anttila et al., 2009). For ultrastructural morphometry, sections were examined directly at the electron microscope at 6.000 x magnification by two unaware observers of the particular treatment, in order to distinguish subcellular structures such as mitochondria, autophagy-like vacuoles and apoptotic features (marginalization and condensation of chromatin, apoptotic

bodies). Each grid contained non serial sections, and for each grid we observed an average of fifty cells. Several grids were observed in order to obtain a total number of 1.000 cells for each experimental group.
In plain microscopy we counted: i) the total number of mitochondria per cell; ii) the number of altered mitochondria per cell; iii) the total number of autophagy-like vacuoles per cell; iv) the number of apoptotic cells.
In order to characterize an altered mitochondrion, we considered the following parameters: i) matrix dilution extending from a small mitochondrial area up to the entire mitochondrial area; ii) the presence of disarranged and/or fragmented cristae. The percentage of altered mitochondria was determined by counting the number of abnormal organelles out of the total number of mitochondria (Fornai et al., 2008).
Both multiple membranes (autophagosomes) containing cytoplasmic material and electrondense membranous structures were scored as autophagy-like vacuoles according to previous studies (Fornai et al., 2004). We counted the number of autophagy-like vacuoles for each cell, and then we calculated the mean value per cell. The count of the number of apoptotic cells in the different groups was performed evaluating 20 grids (about 50 cells per grid). Data were analyzed using ANOVA with Sheffè's post hoc analysis.

Count of immunogold particles

Measurement of the amount of immunogold particles (10 nm or 20 nm) was carried out at electron microscope at 15.000 X magnification by two unaware observers of the particular treatment. The count of immunogold particles localized in the cytosol, mitochondria, and various membranous compartments (endoplasmic reticulum and autophagy-like vacuoles) was obtained from two plastic blocks randomly chosen from each experimental group. These blocks were cut and non-serial ultrathin sections (leaving a space of a few micrometers from each other) were collected. Since biological structures vary in appearance depending upon position and orientation, these considerations can be overcome by using a cell pellet in which each cell can be found in every position and orientation. In this way every orientation of the specimen has an equal chance of being selected. This allowed us to observe the structures of interest independently of their placement in a specific cytoplasmic region. Despite such remarkable variability in appearance due to placement and orientation, results obtained from cell pellets were highly replicable with small variations and minimal standard error.
The count of immunogold particles was performed as described (Lucocq et al., 2004). This method allows counting directly at the TEM by selecting the minimum magnification (15.000x) at which gold particles and cell compartments can be clearly identified. We chose to randomly select a grid square that contained labeled cells. In particular, starting at a grid square corner, the whole of the sectioned pellet within that grid square was scanned continuously in equally spaced parallel sweeps across the specimens. Random selection ensures that scanning was done irrespective of the amount of cell or the intensity of gold labeling. For each group of treatment, we examined 20 grids and counted about 50 cells per grid. For beclin1 and parkin, in each cell we counted the number of anti-beclin1 or anti-parkin immunogold particles localized on mitochondria, and we expressed the mean value of mitochondrial immunogold particles for cell out of 1.000 cell counted (i.e. total number of immunogold particles on the total number of mitochondria in a given cell). For co-localization, we counted the mitochondria that possessed both immunogold particles (10 nm for beclin1 and 20 nm for parkin).
For ubiquitin assessment, we counted in each cell the number of immunogold particles localized at mitochondria, expressed as the mean value of mitochondrial immunogold particles for cell out of 1.000 cell counted. When referring to ubiquitin placement at mitochondria, we intend immunogold particles placed close-by, at a maximal distance of 20 nm (corresponding to the diameter of the gold particle). This was done quite differently compared with the count of parkin and beclin1, since ubiquitin was consistently found outside the outer mitochondrial membrane. Remarkably, the higher was the number of ubiquitin immunostaining, the closer was the placement of the gold particles to the mitochondrial outer membrane (between 0 and 20 nm). LC3 was counted both on autophagy vacuoles (identified as reported above, arrows in Fig. 9A-C, D), on endomembranous structures which were identified mostly as endoplasmic reticulum, and on less defined single membrane structures (arrowheads in Fig. 9B).

Results

PINK1 affects the percentage of altered mitochondria (Figs. 1, 2)

As shown in representative pictures of Fig. 1, modulation of PINK1 expression in PC12 cells produced dramatic changes in the mitochondrial network. In baseline conditions, well conformed elongated mitochondria were observed in control cells as well as in cells overexpressing PINK1wt, while both shPINK1 and PINK1^{W437X} cells showed the presence of clearly altered mitochondria (Figs. 1A-D). The analysis of these experiments by ultrastructural morphometry counts is reported in Fig. 2. We found that PINK1wt overexpressing cells, despite possessing a significantly higher number of mitochondria, did not differ from control cells for the percentage of altered mitochondria counted in baseline conditions. In contrast, PINK1 silenced cells showed a marked increase in the proportion of damaged mitochondria per cell, even with the total number of mitochondria being similar to controls. The percentage of damaged mitochondria was increased also in PINK1^{W437X} cells, although to a lesser extent (Figs. 2A, B). These effects were magnified when the cells were exposed to METH (Figs. 1E-H), which *per se* did not affect the total number of mitochondria, but was able to significantly raise the percentage of damaged mitochondria in control cells (Figs. 2C, D). Upon METH exposure, the number of mitochondria in PINK1wt overexpressing cells was comparable to that seen in baseline condition, but we failed to observe the increase of damaged mitochondria seen in control cells. Conversely, PINK1^{W437X} and even more shPINK1 cells possess a markedly higher percentage of damaged mitochondria, despite their overall number being comparable to controls (Figs. 2E, F). These results suggest that the modulation of PINK1 expression levels affects the homeostasis of mitochondria both in baseline conditions and following METH exposure.

PINK1 modulates the mitochondrial recruitment of beclin1 and parkin and their colocalization at the mitochondrial level (Figs. 3-6)

Since we had previously shown that PINK1 interacts with beclin1, an essential autophagy-initiating molecule, we next asked whether beclin1 could also play a role in the activation of mitophagy, and counted the accumulation of beclin1 particles at mitochondrial level. Representative pictures of the localization of beclin1 immunogold particles in cells overexpressing PINK1wt, in basal condition and upon METH treatment, are shown in Fig. 3. The immunogold counting in Fig. 4 shows the percentage of beclin1-positive mitochondria and the mean number of immunogold-stained beclin1 molecules at mitochondria level. In PINK1wt cells, a significant increase in beclin1-positive mitochondria and in the number of mitochondrial beclin1 particles was counted compared to control cells in baseline conditions. In contrast, the mitochondria localization of beclin1 and the number of beclin1 particles per mitochondrion were significantly reduced in both shPINK1 and PINK1^{W437X} cells (Figs. 4A, B). METH administration per se did not affect the percentage of beclin1-positive mitochondria in control cells, but increased about three folds the number of mitochondrial beclin1 immunogold particles (Figs. 4C, D). Upon METH exposure, PINK1wt overexpression was able to significantly raise both the amount of beclin1-positive mitochondria and the mean number of beclin1 mitochondrial particles compared to control cells, while both values were markedly lower than controls in PINK1^{W437X} and PINK1 silenced cells (Figs. 4E, F).

It has been recently shown that, under mitochondrial depolarization, PINK1 recruits parkin to dysfunctional mitochondria in order to activate mitophagy (Narendra and Youle, 2011). To verify this mechanism in our system, we then measured the accumulation of parkin at mitochondria level. In control cells, the mitochondria localization of parkin was evident as immunogold particles placed both on the outer mitochondrial membrane (Fig. 5A) and mitochondrial cristae (Fig. 5B), and this localization did not significantly change upon modulation of PINK1 expression (data not shown). The percentage of parkin-positive mitochondria in control cells markedly increased upon METH exposure (Fig. 5D). Interestingly, PINK1wt overexpression did not result in any relevant difference in parkin accumulation at the mitochondria compared to control cells; however, mutant or silenced PINK1 cells possessed a significantly lower amount of immunogold-stained parkin at mitochondrial level, both in baseline conditions and following METH exposure (Figs. 5C-E).

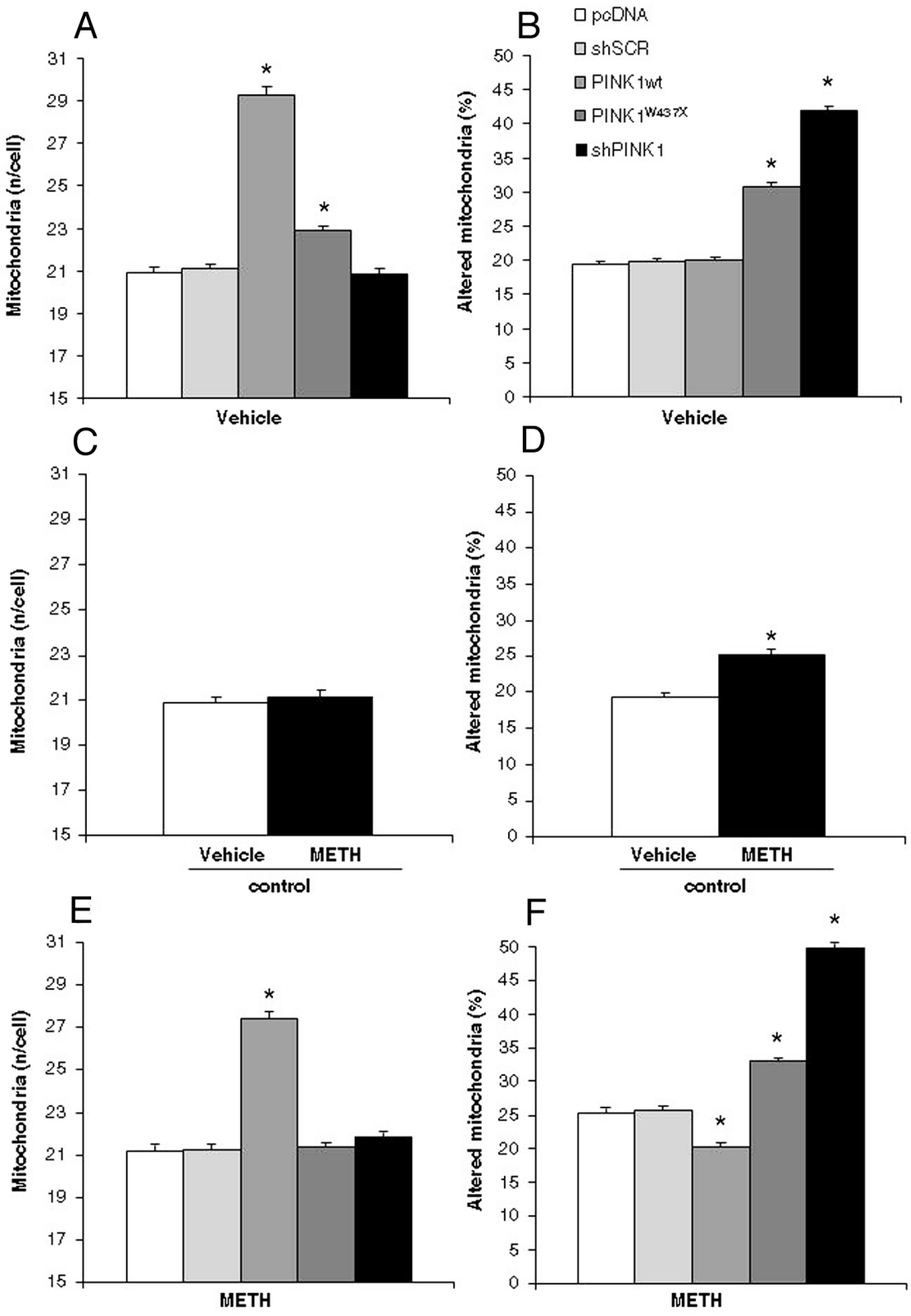

Fig. 2. - PINK1 expression affects the proportion of altered mitochondria.
Graphs indicate the effect of PINK1 modulation upon the total number of mitochondria per cell and the percentage of altered mitochondria both in baseline conditions (A, B, respectively) and after METH exposure (E, F, respectively). The effects of METH administration *per se* in control (untransfected) cells is shown in graphs C and D. * $p < 0.001$ *vs.* other groups.

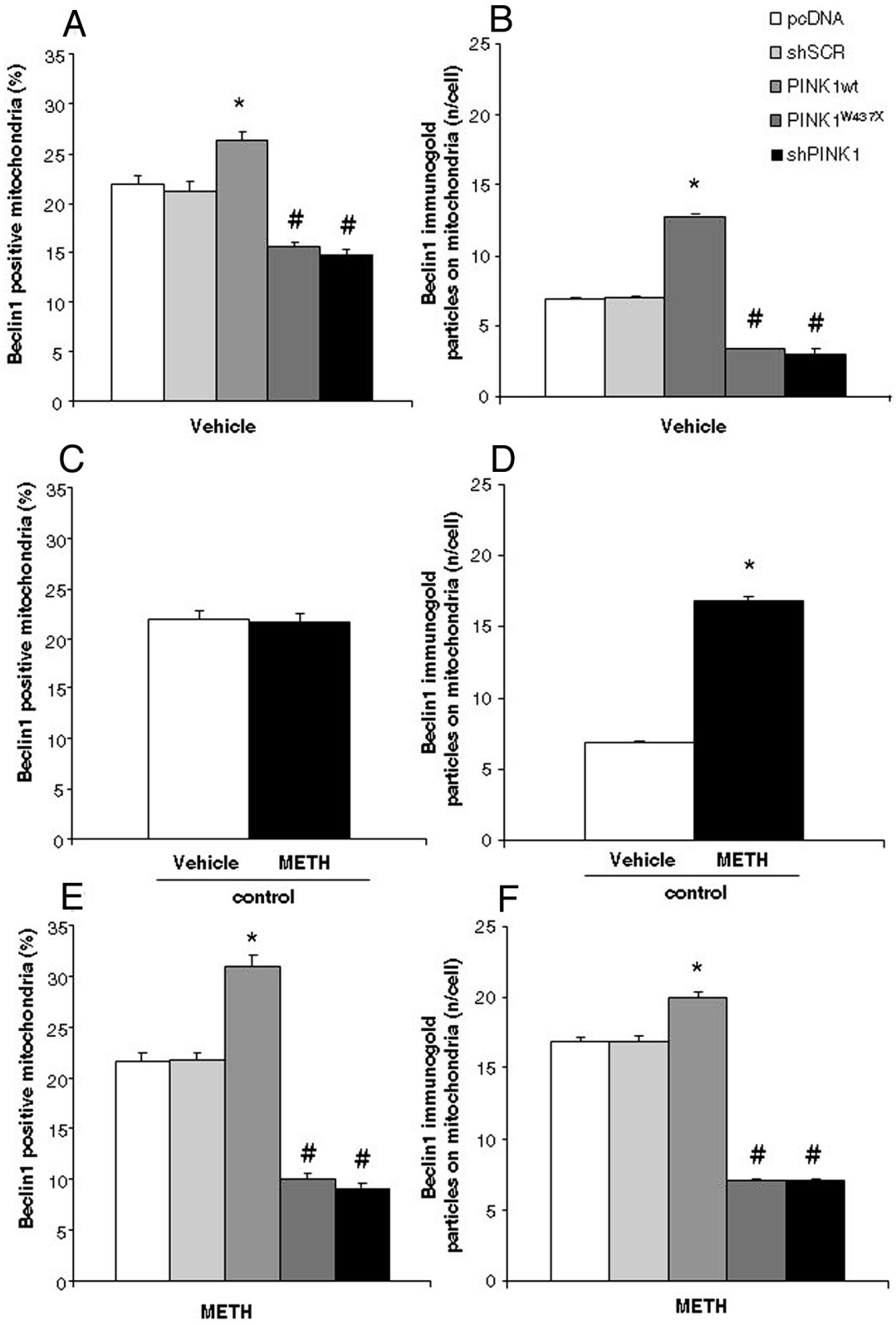

Fig. 3. - PINK1 modulates the recruitment of beclin1 at mitochondrial level.
Graphs indicate the effect of PINK1 modulation upon the percentage of beclin1 immunostained mitochondria and the mean number of immunogold-stained beclin1 molecules at mitochondrial level, both in baseline conditions (A, B) and after METH exposure (E, F). Graphs C, D show the effect of METH administration on both parameters in untransfected cells. * $p < 0.001$ *vs.* other groups; # $p < 0.001$ *vs.* pcDNA/shSCR and PINK1wt.

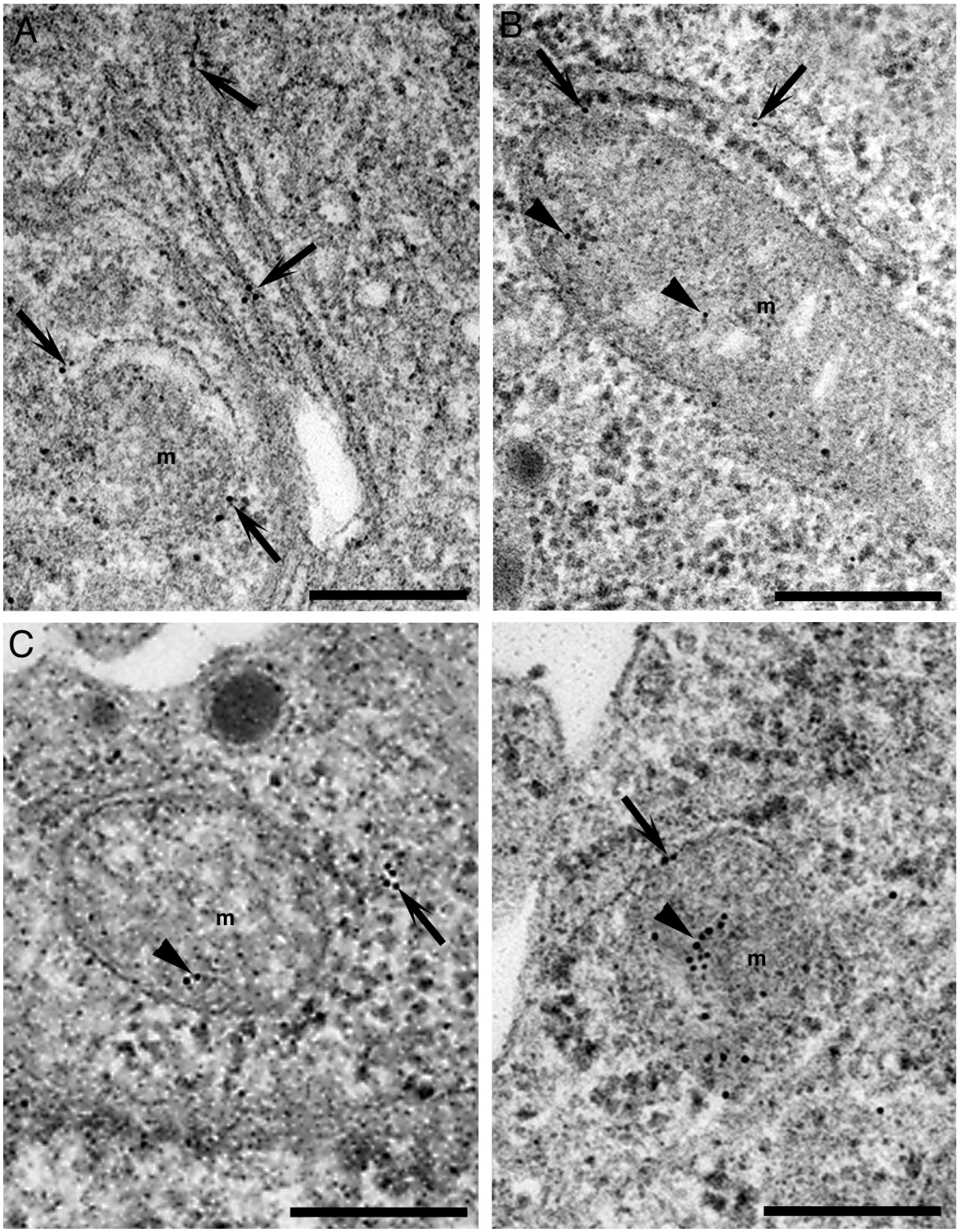

Fig. 4. - Representative localization of beclin1 in PINK1wt overexpressing cells.
Cells overexpressing PINK1wt in baseline conditions (A, B) and upon METH exposure (C, D). A) Anti-beclin1 immunogold particles (10 nm, arrows) are localized on endoplasmic reticulum (ER) cisterns and on membranes that tightly surround a mitochondrion. B) Beclin1 immunogold particles (arrows) on a cistern of rough ER close to a mitochondrion in which gold particles are localized on the cristae (arrowheads). C) A cluster of anti-beclin1 immunogold particles, surrounded by a membrane (arrow), and single gold particles on mitochondrial cristae (arrowhead) are visible; D) anti-beclin1 gold particles on mitochondrial cristae (arrowhead) and on the inner mitochondrial membrane (arrow). m = mitochondrion. Scale bars: 0.25 μm.

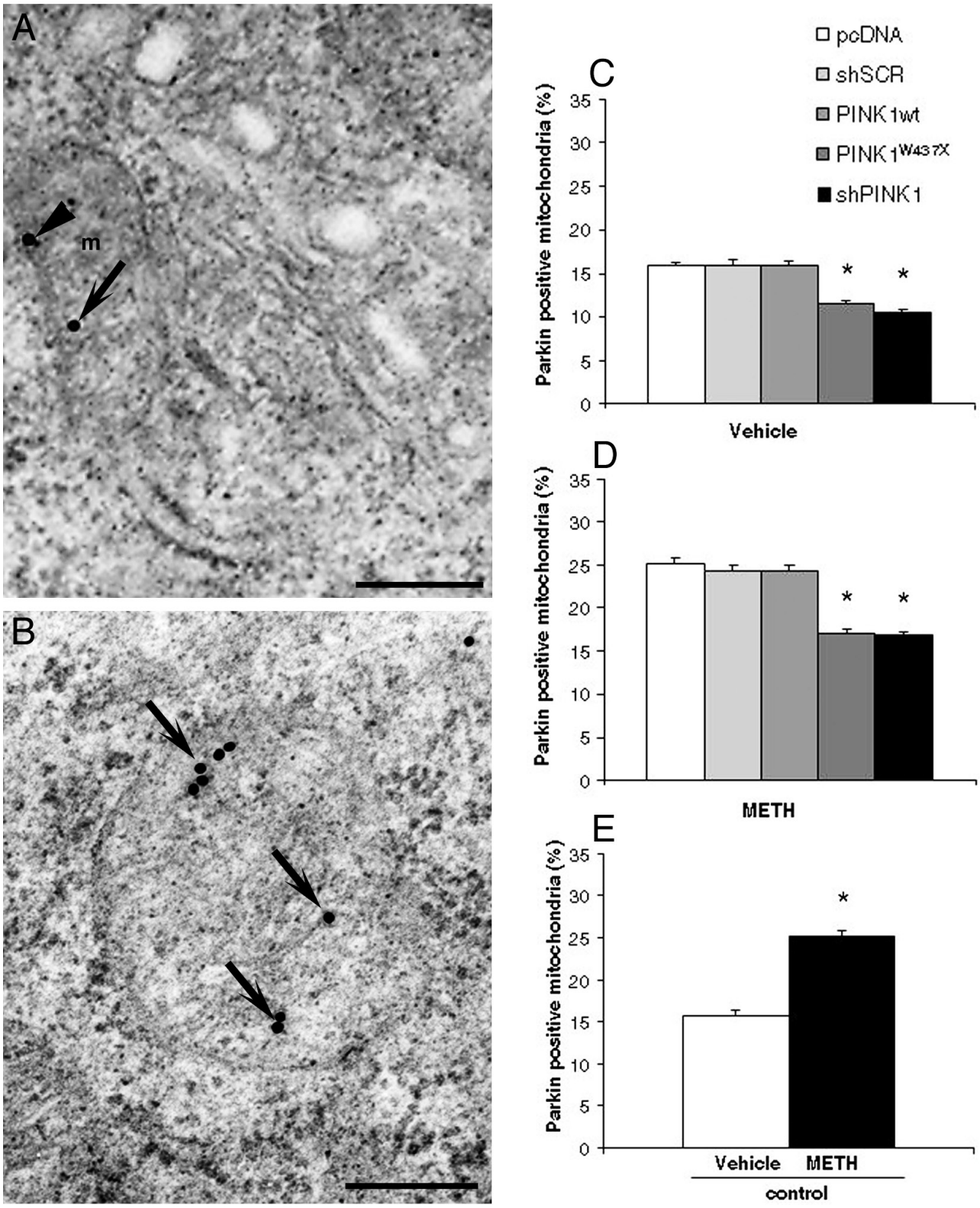

Fig. 5. - PINK1 modulates the recruitment of parkin at mitochondrial level.
A and B are representative images from control cells in basal conditions showing anti-parkin immunogold particles localized on the outer mitochondrial membrane (arrowhead) and on mitochondrial cristae (arrows). Graphs C-E show the effects of PINK1 modulation upon the percentage of parkin-positive mitochondria in baseline conditions (C) and after METH exposure (E), as well as the effect of METH exposure *per se* in control cells (D). * $p < 0.001$ *vs.* pcDNA/shSCR and PINK1wt (C and E), or *vs.* vehicle (D). m = mitochondrion; Scale bars: 0.25 μm.

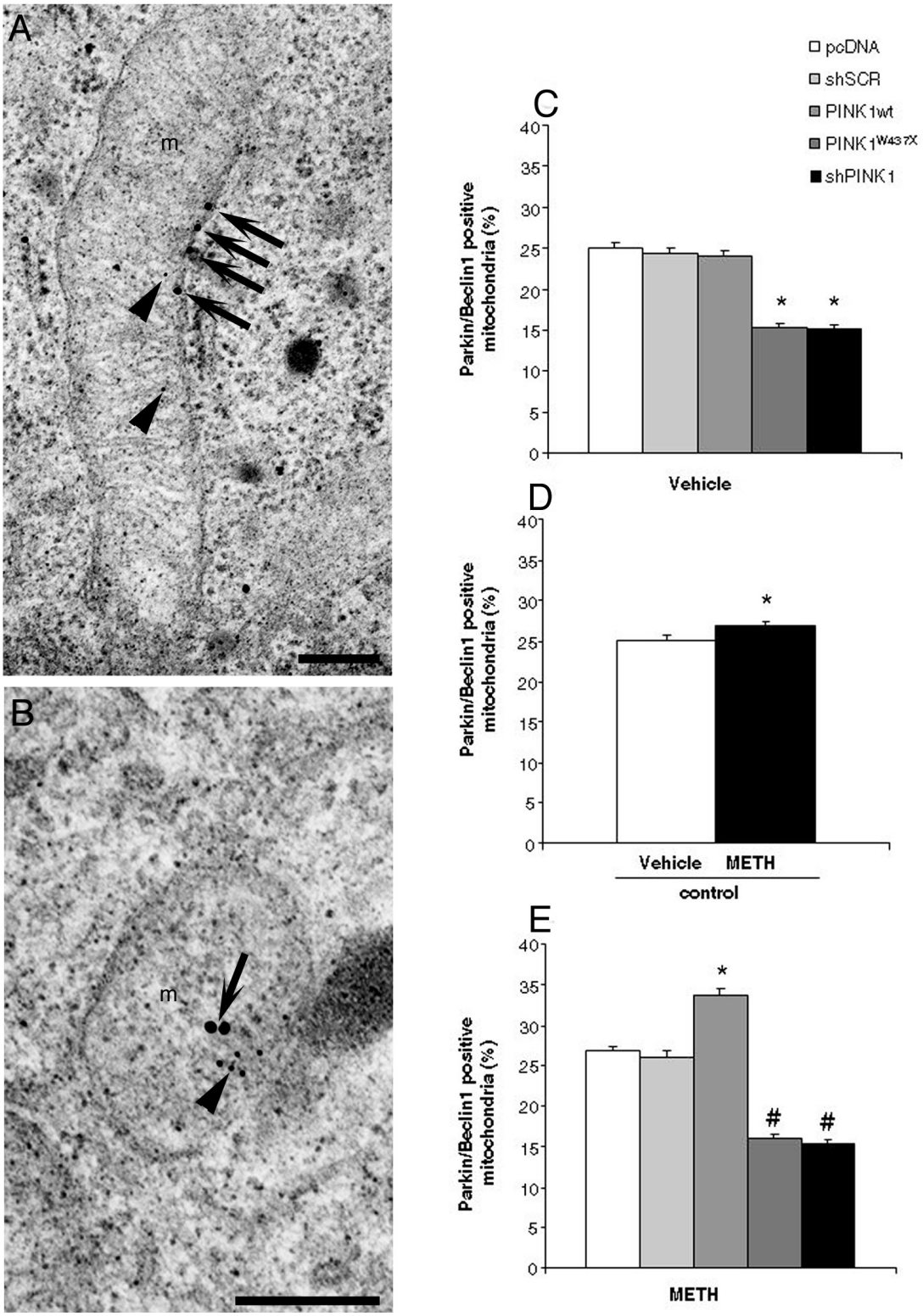

Fig. 6. - PINK1 expression modifies beclin1/parkin co-localization at mitochondria level.
A and B are representative micrographs of METH-treated PINK1wt overexpressing cells. Anti-parkin immunogold particles (20 nm) are distributed on the outer and inner mitochondrial membrane and on the cristae (arrows), while anti-beclin1 immunogold particles (10 nm) are mostly localized on the cristae (arrowheads). Graphs C-E show the mean number of parkin-beclin1 positive mitochondria in baseline conditions (C) and after METH exposure (E), as well as the effect of METH exposure *per se* in untransfected cells (D). * $p < 0.001$ *vs.* other groups, # $p < 0.001$ *vs.* pcDNA/shSCR and PINK1wt. m = mitochondrion; Scale bars: 0.25 μm.

Since PINK1 is known to interact with both beclin1 and parkin, we hypothesized that these two proteins could co-localize in presence of PINK1 to promote mitochondrial removal. To test this hypothesis, we further counted those mitochondria which were concomitantly positive for beclin1 and parkin immunogold staining. As shown in representative pictures (Figs. 6A, B), parkin and beclin1 were found to lie in close proximity both on the outer and inner mitochondrial membrane, and this co-localization was slightly increased upon METH exposure in control cells (Fig. 6D). No difference in the submitochondrial localization of parkin and beclin1 was observed among groups (data not shown). However, we found that the number of mitochondria positive for both beclin1 and parkin was significantly affected by PINK1 modulation. In fact, upon PINK1wt overexpression, METH exposure significantly increased the number of parkin/beclin1 positive mitochondria compared with controls. In contrast, the number of mitochondria immunostained for both parkin and beclin1 markedly dropped in both PINK1^{W437X} and shPINK1 cells, both in baseline conditions and after METH (Figs. 6C, E).

These findings indicate that functional PINK1 determines the accumulation of parkin and beclin1 at the level of the very same mitochondria, and suggest that these proteins likely work in concurrence to trigger the mitophagy process.

PINK1 modulates the mitochondrial clusterization of ubiquitin (Figs. 7, 8)

When recruited to dysfunctional mitochondria, parkin is known to ubiquitinate several proteins of the outer mitochondrial membrane. To assess whether mitochondrial ubiquitination was affected by manipulation of PINK1 expression, we counted the particles of immunogold-stained ubiquitin clustered at mitochondria. We found that the number of ubiquitin particles was markedly influenced by PINK1 levels (Fig. 7). In untreated cells, we observed scarce mitochondrial ubiquitin clusters that only slightly increased upon METH treatment (Fig. 8B). In baseline conditions, the overexpression of PINK1wt but also, unexpectedly, of PINK1^{W437X} increased mitochondrial clusteres of ubiquitin. Conversely, ubiquitin particles significantly decreased in PINK1 silenced cells (Fig. 8A). Upon METH treatment, the increase of mitochondrial ubiquitin in PINK1wt overexpressing cells was slightly magnified, while overexpression of PINK1^{W437X} produced a paradoxical reversal effect compared to untreated cells, resulting in a severe reduction of ubiquitin particles, that were almost undetectable in PINK1 silenced cells (Fig. 8C). Remarkably, mitochondrial ubiquitin was solely detected at the outer mitochondrial membrane, in sharp contrast with the previously described placement of beclin1 and parkin.

PINK1 modulates autophagy-like vacuoles only upon METH exposure (Figs. 9, 10)

To investigate whether the recruitment of beclin1, parkin, and ubiquitin by PINK1 to damaged mitochondria were related to activation of the mitophagy cascade, we carried out a sub-subcellular quantification of autophagy vacuoles by plain electron microscopy. We observed that only some autophagy-like vacuoles were positive for LC3 staining, despite their very similar morphology (Fig. 9A). This may depend on the dynamic state of the autophagy vacuoles, but it is also likely that the ultrathin section may or may not include an area sufficient to stain LC3 particles (see Methods). In some cases, we observed LC3-positive membranes of the endoplasmic reticulum (endomembranous structures) surrounding an altered mitochondrion, that are highly suggestive for mitophagy (Fig. 9B). Representative Figs. 9C, D show the localization of LC3 on membranes of autophagy vacuoles at earlier maturation stages than those presented in Fig. 9A. These figures indicate how LC3 particles were counted on endomembranous structures and autophagy-like vacuoles.

In untreated cells, PINK1 modulation produced no significant differences in either the total number of autophagy-like vacuoles, of those stained for LC3, or of LC3 immunogold particles on endomembranous structures (Figs. 9E and 10A, B). METH exposure induced *per se* a significant increase of all these counts in control cells (Figs. 9F and 10C, D), that remained unchanged in cells overexpressing PINK1wt. Conversely, a significant decrease of all counts was observed in PINK1^{W437X} cells and, even more, in PINK1 silenced cells (Fig. 9G and 10E, F). These data indicate a similar effect for LC3-positive and non-stained autophagy-like vacuoles, that is appreciable only upon stressing conditions in cells lacking a functional PINK1 protein.

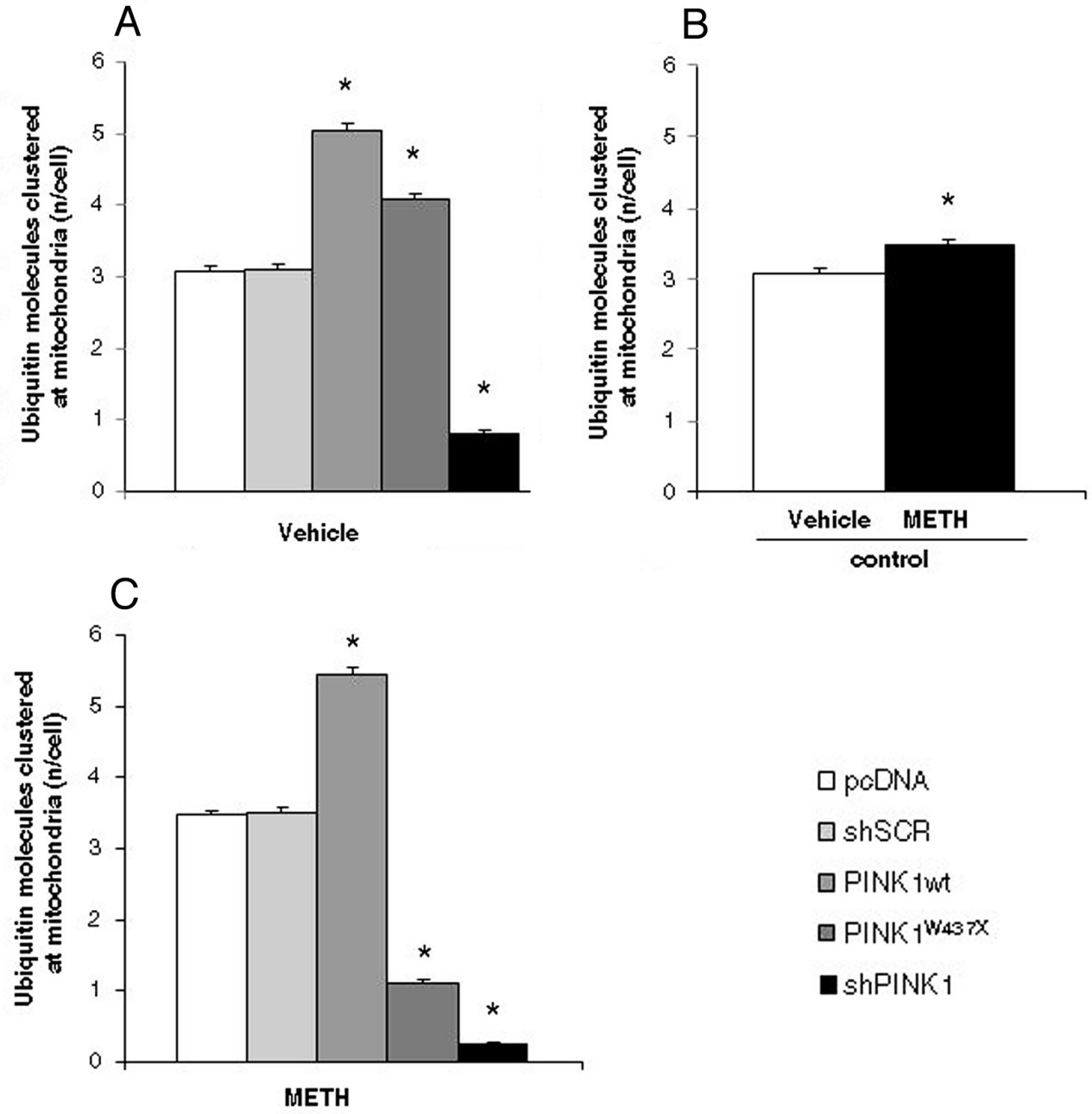

Fig. 7. - PINK1 modifies the number of ubiquitin clusters at mitochondrial level.
Graphs show the mean number of ubiquitin molecules clustered at the mitochondrial level in baseline conditions (A) and after METH exposure (C), as well as the effect of METH exposure in control cells (B). * $p < 0.001$ *vs.* other groups.

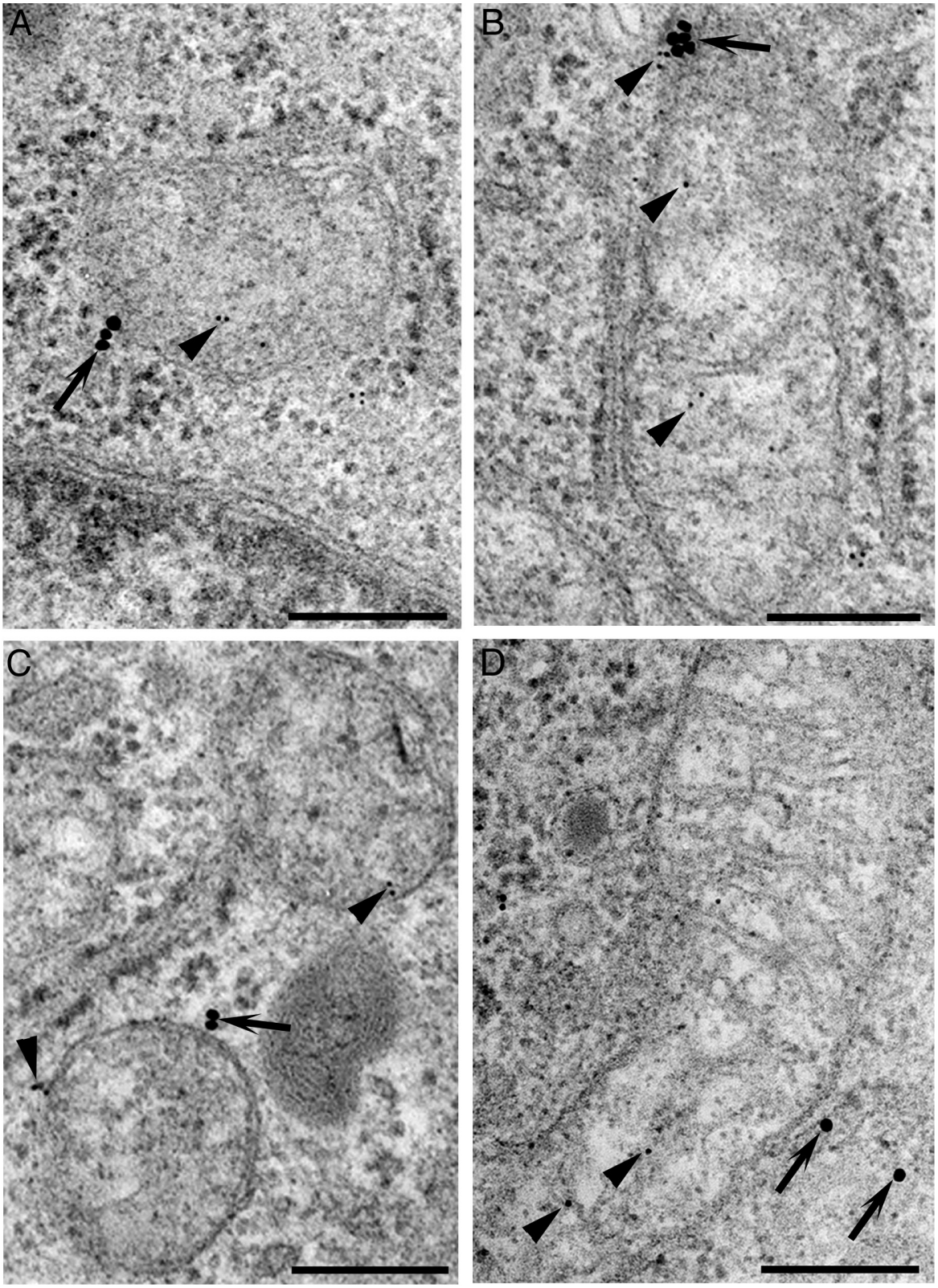

Fig. 8. - PINK1 modulates clustering of ubiquitin at mitochondrial level.
A-D are representative pictures of cells treated with METH, showing clusters of ubiquitin immunogold particles (20nm, arrows) localized near the outer mitochondrial membrane in pcDNA cells (A), PINK1wt (B) and PINK1W437X (C), while in shPINK1 cells only single ubiquitin molecules are observed near mitochondria (D). In the same pictures, beclin1 immunogold particles are also indicated (10 nm, arrowheads). Scale bars: 0.25 μm.

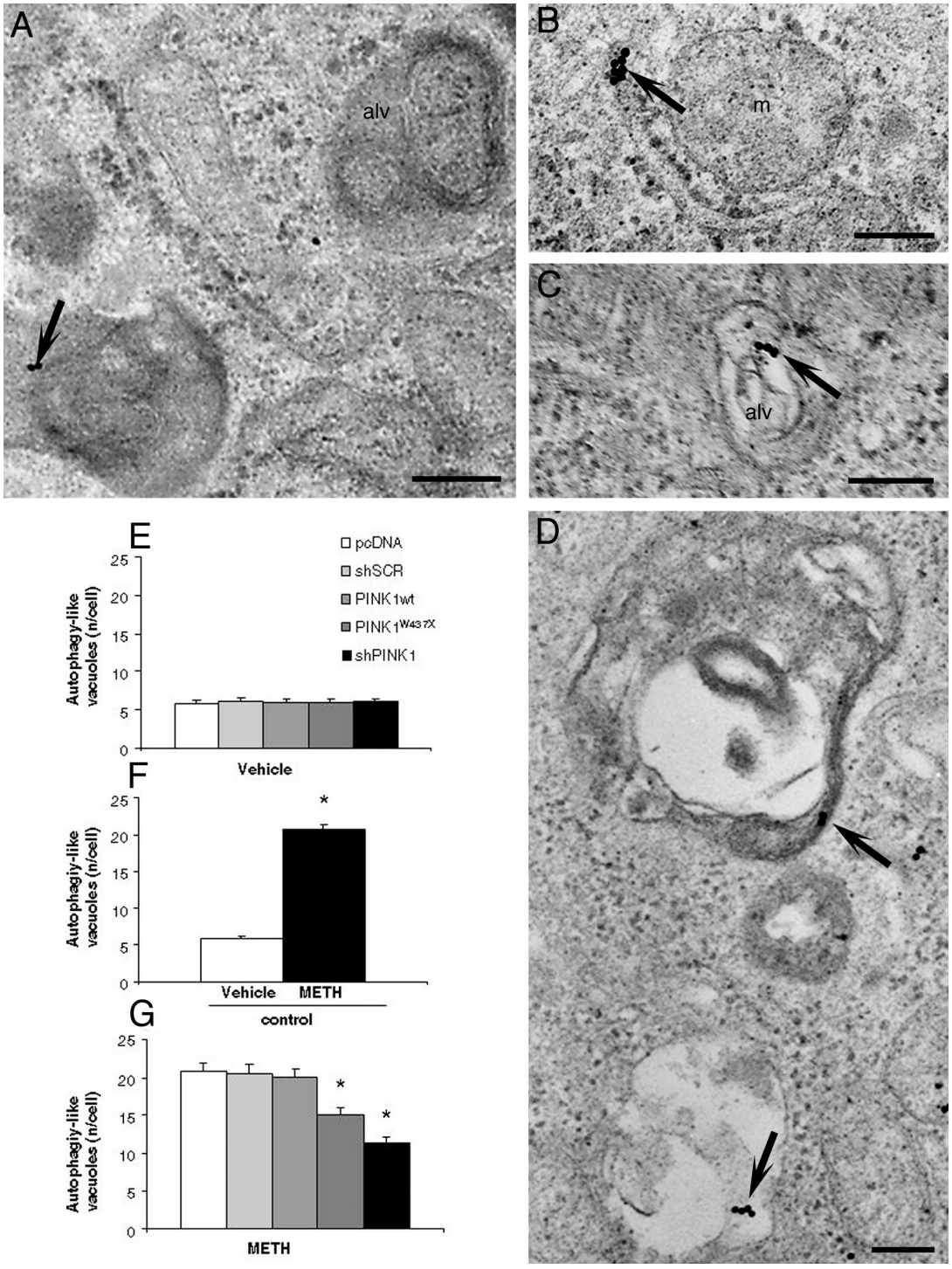

Fig. 9. - PINK1 modulation influences the number of autophagy-like vacuoles within cells.
Micrographs A-D showing representative LC3 positive and negative autophagy-like vacuoles in METH-treated PINK1wt cells. A) On the left an autophagy-like vacuole (alv) possessing anti-LC3 immunogold particles (arrow) is visible; on the right there is an LC3 negative autophagy-like vacuole (alv) containing membranous structures surrounded by ribosome and cytoplasmic material; B) Anti-LC3 immunogold particles (arrow) are localized on the ER surrounding an altered mitochondrion. C) The arrow indicates anti-LC3 immunogold particles localized in the inner membranes of an autophagy-like vacuole at earlier stages of maturation. D) Different stages of maturation of autophagy-like vacuoles exhibiting membranes stained with anti-LC3 immunogold particles (arrows). E, F) Graphs show the mean number of autophagylike vacuoles in baseline conditions (E) and after METH exposure (G), as well as the effect of METH exposure *per se* in control cells (F). * $p < 0.001$ *vs.* other groups. m = mitochondrion, alv = autophagy-like vacuole. Scale bars: 0.25 μm.

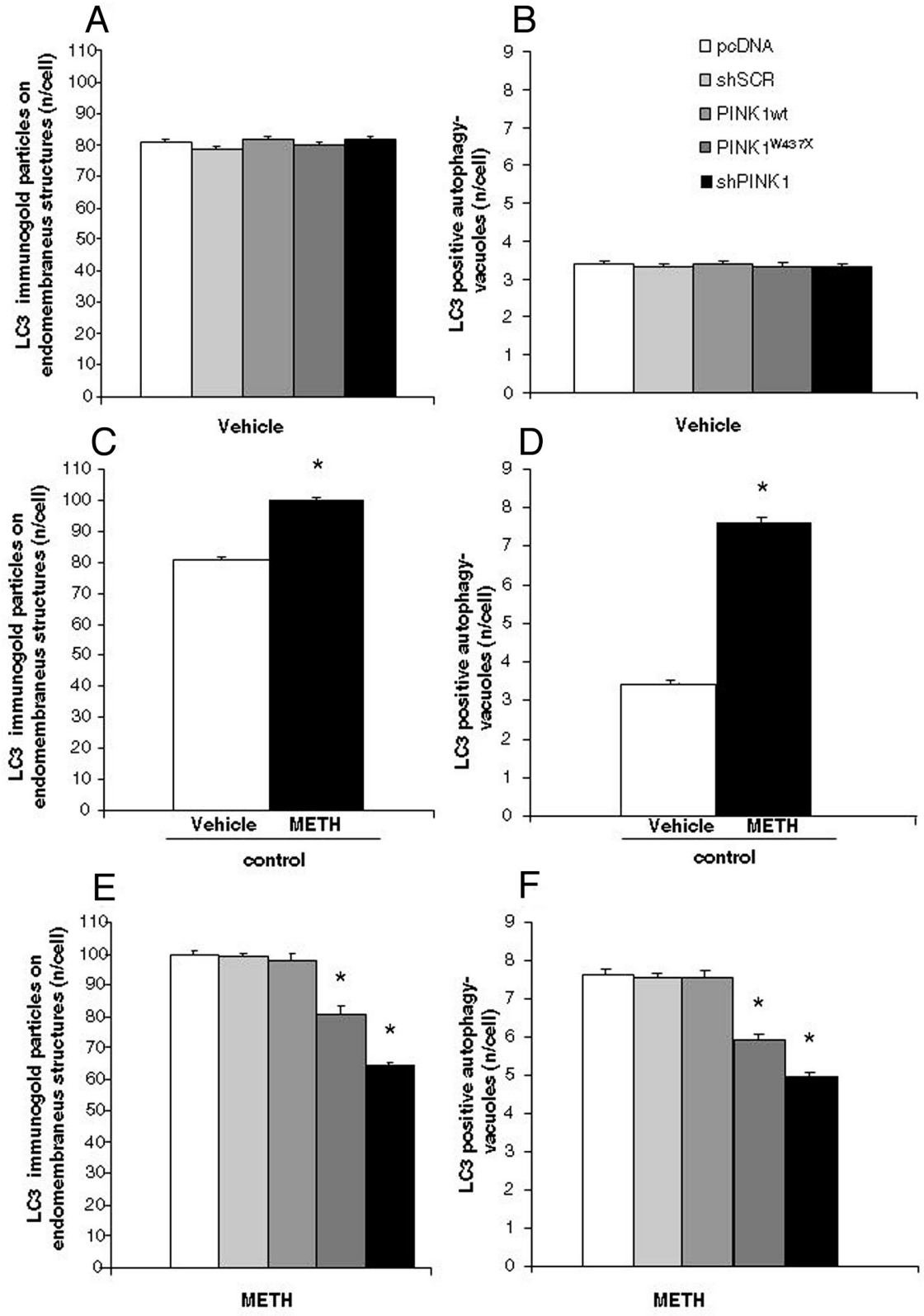

Fig.10. - PINK1 expression modulates the number of LC3-positive structures.
Graphs indicate the effect of PINK1 modulation upon the number of LC3-positive endomembranous structures and the number of LC3 positive autophagy-like vacuoles, both in baseline conditions (A, B) and after METH exposure (E, F). The effect of METH administration *per se* in control cells is shown in graphs C and D. * $p < 0.001$ *vs.* other groups.

PINK1 modulates apoptotic cell death (Fig. 11)

Transmission electron microscopy represents the gold standard not only to discern autophagy structures in the cell, but also to detect apoptosis. We therefore proceeded to count the number of apoptotic cells upon PINK1 modulation, both in baseline conditions and following METH treatment. In fact, it is firmly established that in PC12 cells, METH administration induces typical apoptotic cell death when the autophagy/mitophagy pathway is blocked or impaired (Castino et al., 2008). Representative images are shown in Figs. 11A-D. No change was observed between groups in baseline conditions, where about 5% of cells underwent spontaneous apoptosis; only a slight non-significant decrease of apoptosis was detected in PINK1wt overexpressing cells (Fig. 11E). Following METH exposure, apoptosis increased about two-fold in control cells (Fig. 11F). PINK1wt overexpression resulted in a significant reduction of apoptosis, while in PINK1^{W437X} and PINK1 silenced cells there was a severe enhancement of METH-induced apoptotic cell death (Fig. 11G). Thus, in stressing conditions such as METH, the absence of functional PINK1 causes a dramatic increase in cell death that parallels the disruptive effects of autophagy blockade.

Discussion

The present work indicates that the modulation of PINK1 expression strongly affects mitochondrial homeostasis, and in particular the number of damaged mitochondria. This associates with the concomitant recruitment of beclin1, parkin and ubiquitin at mitochondrial level. This effect, already evident in baseline conditions, becomes critical when the autophagy machinery is severely challenged, as it occurs following METH exposure, when the lack of functional PINK1 leads to a marked increase of apoptotic cell death.

These findings add on published data linking PINK1 and parkin to the activation of mitophagy during mitochondrial depolarization induced by CCCP exposure. In this experimental conditions PINK1 selectively accumulates on the outer membrane of damaged mitochondria, leading to recruitment of parkin, ubiquitination of key mitochondrial proteins and subsequent removal of dysfunctional mitochondria through the autophagy and ubiquitin-proteasome pathways (Chan et al., 2011; Choo et al., 2011; Deas et al., 2011; Narendra and Youle, 2011). Recently, we demonstrated that PINK1 also interacts directly with the pro-autophagy protein beclin1 and positively regulates basal and starvation-induced autophagy (Michiorri et al., 2010). To further assess the function of PINK1 in modulating the autophagy pathway, in the present study we chose to expose catecholamine-containing PC12 cells to methamphetamine (METH), a drug of abuse that is known to produce loss of nigrostriatal dopamine terminals in a variety of animal species including humans (Seiden and Sabol, 1996; Moszczynska et al., 2004; Callaghan et al., 2010) as well as catecholamine cell loss *in vitro* (Cubells et al., 1994; Fornai et al., 2004). METH induces the formation of alpha-synuclein-, parkin- and ubiquitin-positive intracellular vacuoles within nigral dopaminergic cells *in vivo* as well as PC12 cells (Larsen et al., 2002; Fornai et al., 2004). Moreover, METH exposure leads to mitochondrial damage, with decrease of the mitochondrial membrane potential and production of reactive oxygen species (Wu et al., 2007). As a consequence of protein misfolding and mitochondrial damage, cells exposed to METH robustly activate the autophagy pathway to counteract neurotoxicity (Fornai et al., 2004). In fact, we showed that pharmacologically- or genetically-induced autophagy blockade precipitates apoptosis in METH treated cells (Castino et al., 2008).

In the present study, the use of electron microscopy was chosen to allow a direct visualization of (i) the status of mitochondria (both quantitative and qualitative); (ii) the site-specific recruitment of autophagy-related proteins such as beclin1, parkin and ubiquitin, extending the analysis to the mitochondrial co-localization of beclin1 and parkin; (iii) the presence of autophagy vacuoles and endomembranous structures either stained or not stained for LC3; (iv) the occurrence of apoptotic cell death. As such, the ultrastructural analysis represents a powerful tool to implement previous evidence of these phenomena, that was mainly based on indirect observations.

In baseline conditions, we observed that the most striking effect of PINK1 overexpression was a marked increase in the number of total mitochondria per cell, without affecting the overall percentage of

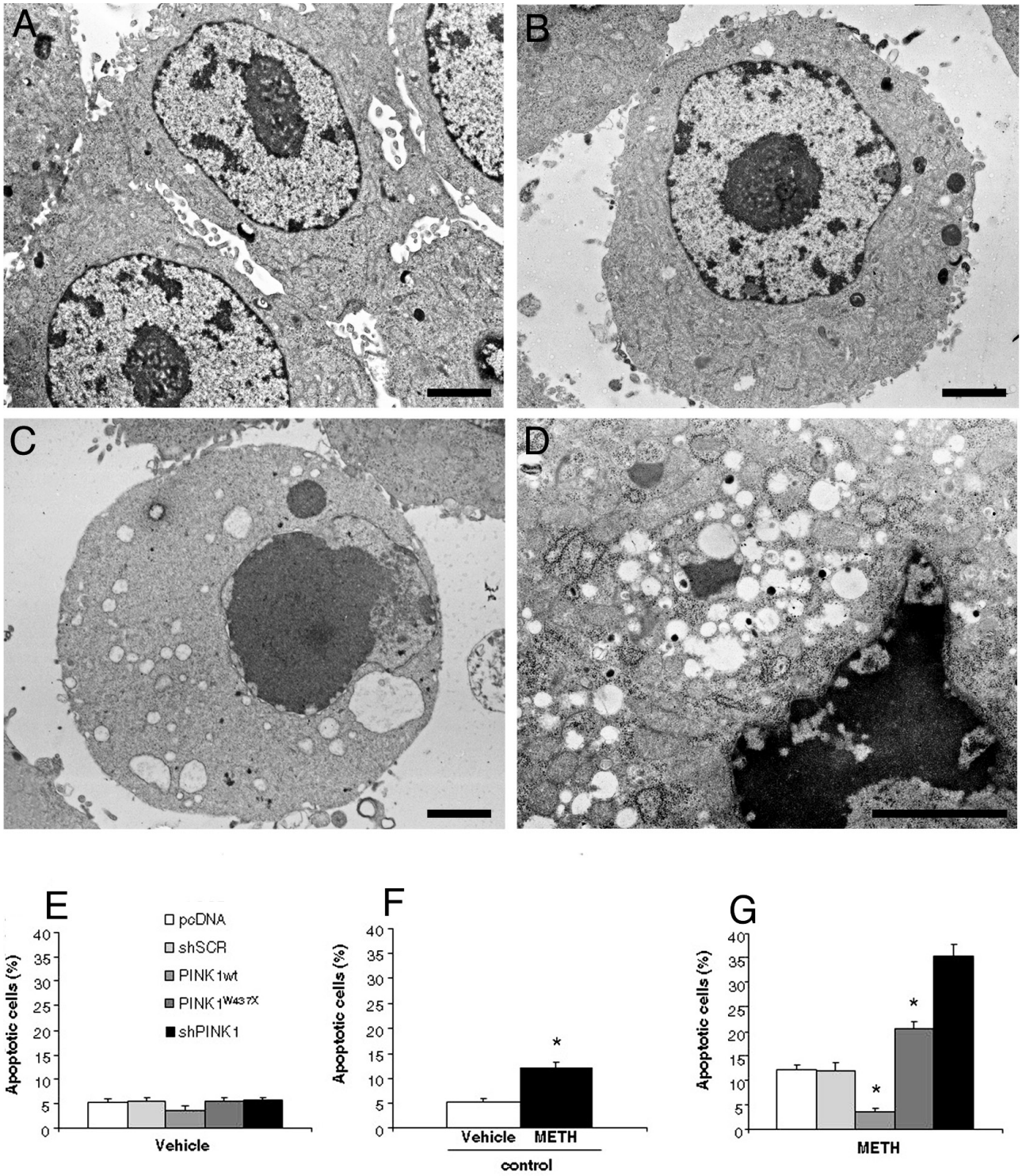

Fig. 11. - PINK1 expression alters METH-induced apoptosis.
A-D are representative pictures after METH exposure. A and B show pcDNA and PINK1wt overexpressing cells, respectively, which possess a normal nuclear and cytoplasmic aspect; C and D show PINK1W437X and shPINK1 cells, respectively. It is evident marginalization and condensation of chromatin, and the presence of apoptotic nuclear body, and vacuolization of cytoplasm. Graphs E-G indicate the effects of PINK1 modulation on the percentage of apoptotic cells both in baseline conditions (E) and after METH exposure (G), and the effects of METH administration *per se* in control cells (F). * $p < 0.001$ *vs.* other groups. Scale bars: 2.0 μm.

damaged mitochondria (about 20%). This finding, that persisted upon METH exposure, implies a possible effect of PINK1 on regulation of mitochondria dynamics. This could be related to a PINK1-induced potentiation of mitochondrial fission, as shown by previous evidences in cellular and *Drosophila* models (Deng et al., 2008; Yang et al., 2008; Dagda et al., 2009). Moreover, it is known that PINK1-related mitochondrial recruitment of parkin leads to the ubiquitination of mitofusin1 and 2, with consequent impairment of mitochondria fusion (Gegg et al., 2010; Poole et al., 2010). This would be in line with our observation of significantly increased levels of mitochondrially clustered ubiquitin upon PINK1 overexpression. Interestingly, we failed to observe a parallel increase in the proportion of parkin-positive mitochondria in PINK1 overexpressing cells versus controls, suggesting that PINK1 could liaise with other, still unknown ubiquitin-ligase proteins or other parkin-independent molecular pathways to bring ubiquitin molecules to mitochondria. Alternatively, it is possible that the marked increase of well conformed mitochondria observed upon PINK1 overexpression could depend on a specific effect of PINK1 in regulating mitochondriogenesis. A recent work based on quantitative methods reported an excess of mitochondrial fission versus fusion in healthy neuronal processes, demonstrating that this imbalance is compensated by a specific growth of the mitochondrial biomass, and that a deficit of this process may be a critical step of neuronal dysfunction leading to neurodegeneration (Berman et al., 2009). It could be speculated that PINK1 could play a role in this process, but this hypothesis should be specifically addressed with quantitative measurements of mitochondrial biomass in presence of different PINK1 expression levels.

Another original finding of this study was that PINK1 overexpression increased the proportion of beclin1-positive mitochondria and raised the number of beclin1 particles clustered at the mitochondrial level. This observation fits well with our previous data showing a direct interaction between PINK1 and beclin1 both in basal conditions and upon autophagy stimuli such as starvation (Michiorri et al., 2010) and suggests a novel, intriguing role for beclin1 in regulating mitophagy. In fact, previous work has focused on the role of beclin1 as a key autophagy-initiating protein promoting the formation of the autophagosome from the endoplasmic reticulum (Pattingre et al., 2005; Kang et al., 2011) while its recruitment and function at the mitochondrial level still remains to be elucidated.

Upon METH exposure, PINK1 overexpression produced a further increase of beclin1 and ubiquitin recruitment at mitochondria, with reduced proportion of damaged mitochondria and decreased apoptosis. These findings confirm the robust protective effect of PINK1 on mitochondrial homeostasis, that is especially evident in conditions of cellular stress such as treatment with METH (Tian et al., 2009).

In line with this, in our experimental system PINK1 silencing produced dramatic effects in PC12 cells even in baseline conditions. In particular, we observed a significant reduction of beclin1, parkin and ubiquitin clustered at mitochondrial level and a subsequent marked increase in the proportion of abnormal mitochondria. Remarkably, data on mitochondrial placement of beclin1 are similar to those for parkin, and results remains the same when beclin1/parkin co-localization is measured. This strongly suggests that PINK1 triggers mitochondrial recruitment of both beclin1 and parkin onto the same damaged mitochondria. These observations indicate that, even in basal conditions, the presence of endogenous PINK1 is essential to regulate the fate of damaged mitochondria, by recruiting mitophagy proteins and promoting mitochondrial targeting by autophagy vacuoles. The observed link between parkin and beclin1 at mitochondrial level is of interest and supports previous observations in different experimental systems. For instance, it has been recently shown that K63-ubiquitination of beclin1 is essential to regulate its proautophagy activity (Shi and Kehrl, 2010) and that parkin is able to stimulate beclin1-dependent mitophagy of defective mitochondria in a transgenic mouse model for Alzheimer's disease (Khandelwal et al., 2011).

All the effects related to PINK1 silencing were magnified upon exposure to METH, a situation requiring a full working autophagy pathway for the cell to avoid irreversible damage. In fact, in METH-treated PINK1 silenced cells, the mitochondrial recruitment of ubiquitin, parkin and beclin1 was minimal and we observed severe accumulation of damaged mitochondria and dramatic increase of apoptotic cell death (up to 40% of cells). This scenario was reminiscent of what we had previously described in

METH-treated PC12 cells under pharmacological or genetic autophagy inhibition, which show accumulation of autophagy substrates, mitochondrial impairment, and stagnant autophagy vacuoles leading to a massive activation of the apoptotic cascade (Castino et al., 2008). Thus, a low METH dose producing only limited apoptosis in control cells is converted into a frankly cytotoxic dose when administered to PINK1 silenced cells, confirming the essential neuroprotective role of PINK1.

Interestingly, we observed that the PINK1^{W437X} mutant protein retained some of its activity, as it was still able to increase the number of cell mitochondria, although to a lesser extent than PINK1wt, and its expression led to a less severe accumulation of damaged mitochondria than PINK1 silencing. In PINK1^{W437X} cells, we also observed reduced recruitment of beclin1 to mitochondria, in line with our previous data indicating that this mutant is less able to interact with beclin1 and to induce autophagy (Michiorri et al., 2010), and a mild increase of mitochondrially targeted ubiquitin but not parkin, supporting our hypothesis that other ubiquitin-ligase proteins may be conveyed by PINK1 at the mitochondrial level.

While PINK1 modulation clearly affected the mitochondrial recruitment of mitophagy-initiating proteins such as beclin1 and ubiquitin, its effect on general autophagy markers, such as the number of autophagy-like vacuoles or the number of clustered LC3 molecules, was much less conspicuous. It is worth mentioning that LC3-positive membrane structures and non-stained autophagy-like vacuoles produced overlapping data in our study. This is inherently consistent with the assumption that LC3 immunostaining confirms the autophagy nature of specific organelles (i.e. autophagosomes at different stages), which can be already identified by plain electron microscopy. Only upon conditions of enhanced autophagy as induced by METH exposure, the lack of functional PINK1 resulted in a significantly lowered number of autophagy-like vacuoles and LC3-positive membrane structures. This is in agreement with our previous data showing a significant reduction of autophagy markers in SH-SY5Y cells upon PINK1 silencing or expression of mutant PINK1^{W437X} only in presence of an autophagy stimulus such as starvation (Michiorri et al., 2010) and it confirms a role for PINK1 in regulating the process of autophagosome formation upon increased demand. For instance, upon mitochondrial depolarization, PINK1-mediated recruitment of parkin is known to ubiquitinate various mitochondrial substrates including specific proteins such as p62. This protein provides a directly link between ubiquitinated mitochondrial proteins and LC3 molecules clustered on endomembranous membranes, promoting the engulfment of the damaged mitochondrion within a newly formed autophagosome (Geisler et al., 2010a; Narendra and Youle, 2011).

In conclusion, this work provides strong evidence showing the key role of PINK1 in the compensatory response to counteract mitochondrial damage and apoptotic cell death. This occurs in combination with the simultaneous mitochondrial recruitment of specific proteins, finely tuning the autophagy pathway and the mitochondrial turnover. The significance of the present study likely extends beyond PD, since autophagy is a process which regulates a variety of physiological phenomena in the cell. Moreover, the dramatic effects caused by modulation of PINK1 expression on METH toxicity highlight a potential role of PINK1 in METH abuse.

Finally this work provides robust ultrastructural evidence showing a key role of PINK1 in the modulating mitochondrial damage and apoptotic cell death in baseline conditions and, mostly following methamphetamine.

Acknowledgements

The authors are grateful to Dr Silvia Michiorri, Dr Alessia Bartalucci and Dr Leonardo Settimini for their assistance in selective experiments, to Mr. Claudio Ghezzani for his precious helping in preparing artwork, to Prof. Mario Giusiani for the gentle gift of methamphetamine, and to Prof. Eliezer Masliah for donating the vector containing PINK1 shRNA.

This work was supported with grants from Telethon Foundation (GGP10140 to EMV), Italian Ministry of Health (Ricerca Corrente 2011 to VG, Ricerca Finalizzata Malattie Rare 2009 and Giovani Ricercatori 2010 to EMV), San Paolo Foundation (3893IT/PF 2008.2395 to FF) and Italian Ministry of Health Ricerca Corrente 2011 (IRCCS INM Neuromed to FF).

References

Bendayan M. and Zollinger M. Ultrastructural localization of antigenic sites on osmium-fixed tissues applying the protein A-gold technique. *J. Histochem. Cytochem.*, **31**: 101-109, 1983.

Berman S.B., Chen Y.B., Qi B., McCaffery J.M., Rucker E.B. 3rd, Goebbels S., Nave K.A., Arnold B.A., Jonas E.A., Pineda F.J., Hardwick J.M. Bcl-x L increases mitochondrial fission, fusion, and biomass in neurons. *J. Cell. Biol.*, **184**: 707-719, 2009.

Bowes B. and Maser M. *Artifacts in fixation for TEM.* 1988, New York: Plenum Press.

Braak H., Ghebremedhin E., Rüb U., Bratzke H., Del Tredici K. Stages in the development of Parkinson's disease-related pathology. *Cell Tissue Res.*, **318**: 121-134, 2004.

Callaghan R.C., Cunningham J.K., Sajeev G., Kish S.J. Incidence of Parkinson's disease among hospital patients with methamphetamine-use disorders. *Mov. Disord.*, **25**: 2333-2339, 2010.

Castino R., Lazzeri G., Lenzi P., Bellio N., Follo C., Ferrucci M., Fornai F., Isidoro C. Suppression of autophagy precipitates neuronal cell death following low doses of methamphetamine. *J. Neurochem.*, **106**: 1426-1439, 2008.

Causton, B. *The choice of resins for electron immunocytochemistry.* 1984, Amsterdam: Elsevier.

Chan N.C., Salazar A.M., Pham A.H., Sweredoski M.J., Kolawa N.J., Graham R.L., Hess S., Chan D.C. Broad activation of the ubiquitin-proteasome system by Parkin is critical for mitophagy. *Hum. Mol. Genet.*, **20**: 1726-1737, 2011.

Cherra S.J. 3rd, Dagda R.K., Chu C.T. Review: autophagy and neurodegeneration: survival at a cost? *Neuropathol. Appl. Neurobiol.*, **36**: 125-132, 2010.

Choo Y.S., Tang C., Zhang Z. Critical Role of PINK1 in Regulating Parkin Protein Levels In Vivo. *Arch Neurol.*, **68**: 684-685, 2011.

Cubells J.F., Rayport S., Rajendran G., Sulzer D. Methamphetamine neurotoxicity involves vacuolation of endocytic organelles and dopamine-dependent intracellular oxidative stress. *J. Neurosci.*, **14**: 2260-2271, 1994.

Cui T., Fan C., Gu L., Gao H., Liu Q., Zhang T., Qi Z., Zhao C., Zhao H., Cai Q., Yang H. Silencing of PINK1 induces mitophagy via mitochondrial permeability transition in dopaminergic MN9D cells. *Brain Res.*, **1394**: 1-13, 2011.

D'Alessandro D., Mattii L., Moscato S., Bernardini N., Segnani C., Dolfi A., Bianchi F. Immunohistochemical demonstration of the small GTPase RhoA on epoxy-resin embedded sections. *Micron*, **35**: 287-296, 2004.

Dagda R.K., Cherra S.J. 3rd, Kulich S.M., Tandon A., Park D., Chu C.T. Loss of PINK1 function promotes mitophagy through effects on oxidative stress and mitochondrial fission. *J. Biol. Chem.*, **284**: 13843-13855, 2009.

Deas E., Wood N.W., Plun-Favreau H. Mitophagy and Parkinson's disease: the PINK1-parkin link. *Biochim. Biophys. Acta*, **1813**: 623-633, 2011.

Deng H., Dodson M.W., Huang H., Guo M. The Parkinson's disease genes pink1 and parkin promote mitochondrial fission and/or inhibit fusion in Drosophila. *Proc. Natl. Acad. Sci. USA*, **105**: 14503-14508, 2008.

Fornai F., Piaggi S., Gesi M., Saviozzi M., Lenzi P., Paparelli A., Casini A.F. Subcellular localization of a glutathione-dependent dehydroascorbate reductase within specific rat brain regions. *Neuroscience*, **104**: 15-31, 2001.

Fornai F., Lenzi P., Gesi M., Soldani P., Ferrucci M., Lazzeri G., Capobianco L., Battaglia G., De Blasi A., Nicoletti F., Paparelli A. Methamphetamine produces neuronal inclusions in the nigrostriatal system and in PC12 cells. *J. Neurochem.*, **88**: 114-123, 2004.

Fornai F., Lenzi P., Capobianco L., Iacovelli L., Scarselli P., Lazzeri G., De Blasi A. Involvement of dopamine receptors and beta-arrestin in metamphetamine-induced inclusions formation in PC12 cells. *J. Neurochem.*, **105**: 1939-1947, 2008.

Gegg M.E., Cooper J.M., Chau K.Y., Rojo M., Schapira A.H., Taanman J.W. Mitofusin 1 and mitofusin 2 are ubiquitinated in a PINK1/parkin-dependent manner upon induction of mitophagy. *Hum. Mol. Genet.*, **19**: 4861-4870, 2010.

Gegg M.E. and Schapira A.H. PINK1-parkin-dependent mitophagy involves ubiquitination of mitofusins 1 and 2: Implications for Parkinson disease pathogenesis. *Autophagy*, **7**: 243-245, 2011.

Geisler S., Holmström K.M., Skujat D., Fiesel F.C., Rothfuss O.C., Kahle P.J., Springer W. PINK1/Parkin-mediated mitophagy is dependent on VDAC1 and p62/SQSTM1. *Nat. Cell. Biol.*, **12**: 119-131, 2010a.

Geisler S., Holmström K.M., Treis A., Skujat D., Weber S.S., Fiesel F.C., Kahle P.J., Springer W. The PINK1/Parkin-mediated mitophagy is compromised by PD-associated mutations. *Autophagy*, **6**: 871-878, 2010b.

Gelb D.J., Oliver E., Gilman S. Diagnostic criteria for Parkinson disease. *Arch. Neurol.*, **56**: 33-39, 1999.

Hardy J. Genetic analysis of pathways to Parkinson disease. *Neuron*, **68**: 201-206, 2010.

Isidoro C., Biagioni F., Giorgi F.S., Fulceri F., Paparelli A., Fornai F. The role of autophagy on the survival of dopamine neurons. *Curr. Top Med. Chem.*, **9**: 869-879, 2009.

Kang R., Zeh H.J., Lotze M.T., Tang D. The Beclin 1 network regulates autophagy and apoptosis. *Cell Death Differ.*, **18**: 571-580, 2011.

Khandelwal P.J., Herman A.M., Hoe H.S., Rebeck G.W., Moussa C.E. Parkin mediates beclin-dependent autophagic clearance of defective mitochondria and ubiquitinated A{beta} in AD models. *Hum. Mol. Genet.*, **20**: 2091-2102, 2011.

Larsen K.E., Fon E.A., Hastings T.G., Edwards R.H., Sulzer D. Methamphetamine-induced degeneration of dopaminergic neurons involves autophagy and upregulation of dopamine synthesis. *J. Neurosci.*, **22**: 8951-8960, 2002.

Lesage S. and Brice A. Parkinson's disease: from monogenic forms to genetic susceptibility factors. *Hum. Mol. Genet.*, **18**: R48-59, 2009.

Lucocq J.M., Habermann A., Watt S., Backer J.M., Mayhew T.M., Griffiths G. A rapid method for assessing the distribution of gold labeling on thin sections. *J. Histochem. Cytochem.*, **52**: 991-1000, 2004.

Matsuda N. and Tanaka K. Uncovering the roles of PINK1 and parkin in mitophagy. *Autophagy*, **6**: 952-954, 2010.

Metcalf D.J., Garcia-Arencibia M., Hochfeld W.E., Rubinsztein D.C. Autophagy and misfolded proteins in neurodegeneration. *Exp. Neurol.*, doi:10.1016/j.expneurol.2010.11.003, 2010.

Michiorri S., Gelmetti V., Giarda E., Lombardi F., Romano F., Marongiu R., Nerini-Molteni S., Sale P., Vago R., Arena G., Torosantucci L., Cassina L., Russo M.A., Dallapiccola B., Valente E.M., Casari G. The Parkinson-associated protein PINK1 interacts with Beclin1 and promotes autophagy. *Cell Death Differ.*, **17**: 962-974, 2010.

Moszczynska A., Fitzmaurice P., Ang L., Kalasinsky K.S., Schmunk G.A., Peretti F.J., Aiken S.S., Wickham D.J., Kish S.J. Why is parkinsonism not a feature of human methamphetamine users? *Brain*, **127**: 363-370, 2004.

Narendra D.P., Jin S.M., Tanaka A., Suen D.F., Gautier C.A., Shen J., Cookson M.R., Youle R.J. PINK1 is selectively stabilized on impaired mitochondria to activate Parkin. *PLoS Biol.* **8**: e1000298, 2010.

Narendra D.P. and Youle R.J. Targeting mitochondrial dysfunction: role for PINK1 and Parkin in mitochondrial quality control. *Antioxid. Redox Signal.*, **14**: 1929-1938, 2011.

Pasquali L., Ruggieri S., Murri L., Paparelli A., Fornai F. Does autophagy worsen or improve the survival of dopaminergic neurons? *Parkinsonism Relat. Disord.*, **15 Suppl 4**: S24-27, 2009.

Pattingre S., Tassa A., Qu X., Garuti R., Liang X.H., Mizushima N., Packer M., Schneider M.D., Levine B. Bcl-2 antiapoptotic proteins inhibit Beclin 1-dependent autophagy. *Cell*, **122**: 927-939, 2005.

Pogson J.H., Ivatt R.M., Whitworth A.J. Molecular mechanisms of PINK1-related neurodegeneration. Curr. Neurol. *Neurosci. Rep.*, **11**: 283-290, 2011.

Poole A.C., Thomas R.E., Yu S., Vincow E.S., Pallanck L. The mitochondrial fusion-promoting factor mitofusin is a substrate of the PINK1/parkin pathway. *PLoS One*, **5**: e10054, 2010.

Seiden L.S. and Sabol K.E. Methamphetamine and methylenedioxymethamphetamine neurotoxicity: possible mechanisms of cell destruction. *NIDA Res. Monogr.*, **163**: 251-276, 1996.

Shi C.S. and Kehrl J.H. Traf6 and A20 differentially regulate TLR4-induced autophagy by affecting the ubiquitination of Beclin 1. *Autophagy*, **6**: 986-987, 2010.

Shults C.W. Lewy bodies. *Proc. Natl. Acad. Sci. USA*, **103**: 1661-1668, 2006.

Silvestri L., Caputo V., Bellacchio E., Atorino L., Dallapiccola B., Valente E.M., Casari G. Mitochondrial import and enzymatic activity of PINK1 mutants associated to recessive parkinsonism. *Hum. Mol. Genet.*, **14**: 3477-3492, 2005.

Swanlund J.M., Kregel K.C., Oberley T.D. Investigating autophagy: quantitative morphometric analysis using electron microscopy. *Autophagy*, **6**: 270-277, 2010.

Tian C., Murrin L.C., Zheng J.C. Mitochondrial fragmentation is involved in methamphetamine-induced cell death in rat hippocampal neural progenitor cells. *PLoS One*, **4**: e5546, 2009.

Valente E.M., Abou-Sleiman P.M., Caputo V., Muqit M.M., Harvey K., Gispert S., Ali Z., Del Turco D., Bentivoglio A.R., Healy D.G., Albanese A., Nussbaum R., González-Maldonado R., Deller T., Salvi S., Cortelli P., Gilks W.P., Latchman D.S., Harvey R.J., Dallapiccola B., Auburger G., Wood N.W. Hereditary early-onset Parkinson's disease

caused by mutations in PINK1. *Science*, **304**: 1158-1160, 2004.

Wu C.W., Ping Y.H., Yen J.C., Chang C.Y., Wang S.F., Yeh C.L., Chi C.W., Lee H.C. Enhanced oxidative stress and aberrant mitochondrial biogenesis in human neuroblastoma SH-SY5Y cells during methamphetamine induced apoptosis. *Toxicol. Appl. Pharmacol*, **220**: 243-251, 2007.

Xilouri M. and Stefanis L. Autophagic pathways in Parkinson disease and related disorders. *Expert Rev. Mol. Med.*, **13**: e8, 2011.

Yang Y., Ouyang Y., Yang L., Beal M.F., McQuibban A., Vogel H., Lu B. Pink1 regulates mitochondrial dynamics through interaction with the fission/fusion machinery. *Proc. Natl. Acad. Sci. USA*, **105**: 7070-7075, 2008.

Ylä-Anttila P., Vihinen H., Jokitalo E., Eskelinen E.L. Monitoring autophagy by electron microscopy in Mammalian cells. *Methods Enzymol.*, **452**: 143-164, 2009.

Yoshii S.R., Kishi C., Ishihara N., Mizushima N. Parkin Mediates Proteasome-dependent Protein Degradation and Rupture of the Outer Mitochondrial Membrane. *J. Biol. Chem.*, **286**: 19630-19640, 2011.

Youle R.J. and Narendra D.P. Mechanisms of mitophagy. *Nat. Rev. Mol. Cell Biol.*, **12**: 9-14, 2011.